Hydrogenation of the Central C–C Bond of Coordinated α-Diimine Ligands of $H_2Ru_2(CO)_5(^iPrN{=}C(H)C(R){=}N^iPr)$ (R = H, Me), Involving C–H and Ru–H Bond-Making and -Breaking Processes

Marco J. A. Kraakman, Cornelis J. Elsevier, and Kees Vrieze*

Anorganisch Chemisch Laboratorium, J. H. van 't Hoff Instituut, Universiteit van Amsterdam, Nieuwe Achtergracht 166, 1018 WV Amsterdam, The Netherlands

Anthony L. Spek

Bijvoet Centre for Biomolecular Research, Vakgroep Kristal- en Structuurchemie, RijksUniversiteit Utrecht, Padualaan 8, 3584 CH Utrecht, The Netherlands

Received June 8, 1992

Reaction of $H_2Ru_2(CO)_5(^iPr\text{-}DAB)$ (**2a**) with D_2 at 60 °C yielded $D_2Ru_2(CO)_5(^iPr\text{-}DAB)$ (**2a'**), whereas **2a'** can be reconverted to **2a** by reaction with H_2. The process is not a simple reductive elimination of H_2 followed by oxidative addition of D_2, since ^1H-NMR showed e.g. that the bridging hydride in **2a** is more rapidly substituted by D than the terminal one, whereas in the reverse case the substitution of the bridging deuteride in **2a'** also occurs much more rapidly than the substitution of the terminal D atom. At 90 °C reaction of $H_2Ru_2(CO)_5(^iPr\text{-}DAB)$ (**2a**) with H_2 led to the reduction of the coordinated DAB ligand with formation of $H_2Ru_2(CO)_5(^iPrNCH_2CH_2N^iPr)$ (**3a**) and of $Ru_2(CO)_6(^iPrNCH_2CH_2N^iPr)$ (**4a**), the latter being formed from **3a** by reaction with CO liberated by some decomposition. In the case of $^iPr\text{-}DAB\{H,Me\}$ only $Ru_2(CO)_6(^iPrNC(H)(Me)CH_2N^iPr)$ (**4b**) could be isolated, although the pentacarbonyl derivative $H_2Ru_2(CO)_5(^iPrNC(H)(Me)CH_2N^iPr)$ (**3b**) could be detected spectroscopically as an intermediate. Use of D_2 showed that the reduction reactions, which are completely inhibited by CO, are not stereoselective. For example for the reaction of $D_2Ru_2(CO)_5(^iPr\text{-}DAB)$ (**2a'**) with deuterium, D atoms were found on all four positions of the central C–C bond, whereas the presence of less than one proton on this moiety and the presence of H on the position of the bridging deuteride indicate that C–H, C–D, Ru–H, and Ru–D bond-making and -breaking processes occur in some stage of the reduction process. Single-crystal structure determinations of **3a** and **4a** have been carried out. Crystals of **3a** are monoclinic, space group $P2_1/c$, with a = 9.832 (1) Å, b = 16.164 (2) Å, c = 12.079 (2) Å, β = 109.72 (1)°, and Z = 4. The structure was refined to R = 0.039 for 2535 observed reflections. Crystals of **4a** are orthorhombic, space group $P2_1ab$, with a = 13.741 (1) Å, b = 14.496 (1) Å, c = 19.271 (1) Å, and Z = 8. The structure was refined to R = 0.034 for 4249 observed reflections.

Introduction

Over the last decade much research has been carried out on the preparation and reactivity of α-diimine transition metal complexes.[1,2] Many interesting facets have been reported with regard to the versatile behavior of the α-diimines in transition metal chemistry. A particular interesting aspect is that treatment of the mononuclear $Mn(Br)(CO)_3(R\text{-}DAB)$ (R-DAB{X,Y} = 1,4-diaza-1,3-butadiene, RN=C(X)C(Y)=NR)[3] with $HFe(CO)_4^-$ was shown to lead to dinuclear complexes, accompanied by N–H or C–H bond formation, which reactions proved to be strongly dependent on the R group of the R-DAB ligand.[4,5] When ^{p}Tol-DAB was used, the reaction resulted in an unusual and novel hydrogenation of the DAB ligand, with the formation of $FeMn(\mu\text{-}H)(CO)_6(^pTolNCH_2CH_2N^pTol)$ (Figure 1A) containing a bridging, formally dianionic, diamido ligand $^pTolNCH_2CH_2N^ptol$. Interestingly, the use of $DFe(CO)_4^-$ showed that the two D atoms were added trans toward each other, which reaction proved to proceed very selectively.[5]

Furthermore, it has been reported that treatment of $FeRu(CO)_6(^iPr\text{-}DAB)$ with hydrogen also leads to reduction of the DAB ligand, with the formation of $FeRu(CO)_6(^iPrNCH_2CH_2N^iPr)$[6] (Figure 1B), while again the reaction proceeded very selectively i.e. with trans addition of the D atoms when D_2 was employed.

Attempts have been made to prepare the coordinated diamido ligand $[RNCH_2CH_2NR]^{2-}$ by reaction of the homonuclear complexes $M_2(CO)_6(DAB)$ (M = Fe, Ru) with hydrogen. However, in the case of the Fe_2 system only decomposition was observed whereas for ruthenium first $Ru_2(CO)_5(DAB)$ was formed, which was subsequently followed by an oxidative addition of hydrogen, leading to $H_2Ru_2(CO)_5(DAB)$ (Figure 1C).[7]

In order to gain a better understanding of the factors determining the differences between the homo- and heterodinuclear systems, a more detailed study on the behavior of the homonuclear Ru complexes toward hydrogen was performed. This paper deals with the results of this work, showing that also for the Ru_2 system reduction of the coordinated DAB ligand by H_2 may take place but not

(1) (a) Koten van, G.; Vrieze, K. *Adv. Organomet. Chem.* **1982**, *21*, 151. (b) Vrieze, K. *J. Organomet. Chem.* **1986**, *300*, 307. (c) Vrieze, K.; Koten van, G. *Inorg. Chim. Acta* **1985**, *100*, 79.

(2) Mul, W. P.; Elsevier, C. J.; Frühauf, H.-W.; Vrieze, K.; Pein, I.; Zoutberg, M. C.; Stam, C. H. *Inorg. Chem.* **1990**, *29*, 2336.

(3) In this paper $^iPrN{=}C(H)C(H){=}N^iPr$ (**a**) and $^iPrN{=}C(H)C(Me){=}N^iPr$ (**b**) are used.

(4) Keijsper, J.; Mul, J.; Koten van, G.; Vrieze, K.; Ubbels, H. C.; Stam, C. H. *Organometallics* **1984**, *3*, 1732.

(5) Keijsper, J.; Grimberg, P.; Koten van, G.; Vrieze, K.; Cristophersen, M.; Stam, C. H. *Inorg. Chim. Acta* **1985**, *102*, 29.

(6) Zoet, R.; Duineveld, C. A. A.; Elsevier, C. J.; Goubitz, K.; Heijdenrijk, D.; Koten van, G.; Stam, C. H.; Versloot, P.; Vrieze, K.; Wijnkoop van, M. *Organometallics* **1989**, *8*, 23.

(7) Keijsper, J.; Polm, L. H.; Koten van, G.; Vrieze, K.; Nielsen, E.; Stam, C. H. *Organometallics* **1985**, *4*, 2006.

0276-7333/92/2311-4250$03.00/0

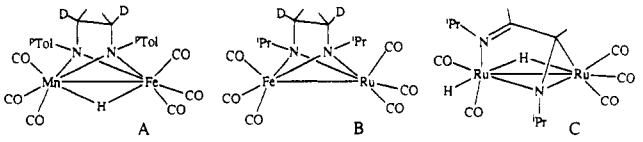

Figure 1. Structures of (μ-H)FeMn(CO)$_5$(ᵖTolNC(H)(D)C(H)(D)NᵖTol) (A), FeRu(CO)$_6$(ⁱPrNC(H)(D)C(H)(D)NⁱPr) (B), and $H_2Ru_2(CO)_5$(ⁱPr-DAB) (C).

in a stereoselective manner as shown by the use of D_2.

Experimental Section

Materials and Apparatus. ^{1}H- and ^{13}C-NMR spectra were recorded on Bruker AC-100, WM-250, and AMX-300 spectrometers. IR spectra (ν(CO) 2200–1600 cm^{-1}) were measured on a Perkin-Elmer 283 spectrometer. Elemental analyses were carried out by the elemental analyses section of the Institute of Applied Chemistry TNO, Zeist, The Netherlands, or by Dornis und Kolbe, Microanalytisches Laboratorium, Mülheim, Germany. All preparations were carried out under an atmosphere of purified nitrogen, using carefully dried solvents. Column chromatography was performed using silica gel (Kieselgel 60, Merck, 70–230 Mesh ASTM, dried and activated before use) as the stationary phase. $Ru_3(CO)_{12}$ (Strem), 2-aminopropane (Merck), PPh_3 (Merck), methylglyoxal (25% aqueous solution; Fluka), D_2 (Air Products), H_2 (Hoekloos, Netherlands), and carbon monoxide (Mattheson) were used as commercially obtained. Me_3NO (Aldrich) was dried before use by heating in vacuo. ⁱPr-DAB was prepared by the condensation reaction of glyoxal and isopropylamine.[8,9] ⁱPr-DAB{H,Me} was prepared by a modified literature procedure as described below. Complexes $Ru_2(CO)_6$(ⁱPr-DAB{H,R}) (R = H (**1a**); R = Me (**1b**)) were prepared by published procedures.[10]

High-pressure NMR experiments were performed using a home built apparatus consisting of a Ti/Al/V pressure head and a 10-mm external and 8.4-mm internal diameter sapphire NMR tube suitable for measurements up to 140 bar of gas pressure.[11] A volume of 1.5 mL of a C_6D_6 solution was syringed into the sapphire tube which was kept under an atmosphere of dinitrogen using a specially designed glass vessel. The tube was then connected to a high-pressure system and pressurized with the desired gas. Subsequently the NMR tube was closed and disconnected from the high-pressure system, and the reaction was monitored by means of NMR spectroscopy.

1. Preparation of ⁱPr-DAB{H,Me}. A mixture of 2-aminopropane (35 mL), hexane (50 mL), and formic acid (5 mL) was stirred at 0 °C while 50 mL of an 25% aqueous solution of methylglyoxal was added dropwise over a period of 15 min. The reaction mixture was stirred at 0 °C for 4 h and at room temperature for an additional 20 h. Subsequently 10 mL of 2-aminopropane was added and the reaction mixture was refluxed for 1 h. The hexane layer was then separated from the aqueous layer, and the latter was extracted with hexane several times. All hexane fractions were then collected, dried over Na_2SO_4, filtered, and evaporated in vacuo, resulting in a yellow oil which was stored at −20 °C. NMR spectroscopy indicated that the oil contained ⁱPr-DAB{H,Me} exclusively. The yield of the reaction usually varied from 40% to 55%. Further purification could be performed by distillation of the oil in vacuo, but this was accompanied by a substantial amount of polymerization.

2. Preparation of $H_2Ru_2(CO)_5$(ⁱPrNCH$_2$CH$_2$NⁱPr) (3a) and $Ru_2(CO)_6$(ⁱPrNCH$_2$CH$_2$NⁱPr) (4a). An amount of 300 mg of $Ru_2(CO)_6$(ⁱPr-DAB) (**1a**) (0.59 mmol) was dissolved in heptane and stirred under an atmosphere of hydrogen (about 1.5 bar) at 90 °C. The hydrogen atmosphere was refreshed regularly, while the conversion was monitored by means of IR spectroscopy. The reaction was stopped when IR spectroscopy indicated that only $H_2Ru_2(CO)_5$(ⁱPrNCH$_2$CH$_2$NⁱPr) (**3a**) and $Ru_2(CO)_6$(ⁱPrNCH$_2$CH$_2$NⁱPr) (**4a**) were left in solution, and the reaction mixture was brought upon a column for purification. Elution with ligroin afforded two poorly resolved pale yellow fractions.[12,13] The first fraction contained mainly **4a** whereas in the second one **3a** was the major component. This reaction route provided complexes **3a** and **4a** in yields of 30% and 40%, respectively.

3. Thermal Conversion of $H_2Ru_2(CO)_5$(ⁱPrNCH$_2$CH$_2$NⁱPr) (3a) to $Ru_2(CO)_6$(ⁱPrNCH$_2$CH$_2$NⁱPr) (4a). An amount of 150 mg of $H_2Ru_2(CO)_5$(ⁱPrNCH$_2$CH$_2$NⁱPr) (**3a**) was dissolved in 20 mL of benzene and refluxed while the reaction was monitored by means of IR spectroscopy. After about 3 h IR spectroscopy indicated that the conversion to $Ru_2(CO)_6$(ⁱPrNCH$_2$CH$_2$NⁱPr) (**4a**) had completed. After evaporation of the solvent and extraction of the residue with hexane **4a** was obtained in about 70% yield.

4. Hydrogenation Reactions of $H_2Ru_2(CO)_5$(ⁱPr-DAB) (2a) with and without Carbon Monoxide. An amount of 300 mg of $Ru_2(CO)_6$(ⁱPr-DAB) (**1a**) was dissolved in 40 mL of heptane and converted to $H_2Ru_2(CO)_5$(ⁱPr-DAB) (**2a**) by treatment with hydrogen at 90 °C.[7] A stream of hydrogen and a stream of carbon monoxide were bubbled through a reverse-flow bubbler with approximately equal velocity and led into a mixing chamber. The gas mixture was then bubbled through the heptane solution of **2a**, while the reaction was monitored by means of IR spectroscopy. After about 5 h at 100 °C IR spectroscopy indicated that still no changes in the composition of the reaction mixture had occurred. Subsequently the stream of carbon monoxide was stopped and only hydrogen was bubbled through the reaction mixture, resulting in a complete conversion to a mixture of **3a** and **4a** within 3 h. Yields of **3a** and **4a** were similar to those of experiment 2.

5. Hydrogenation of $Ru_2(CO)_6$(ⁱPr-DAB{H,Me}) (1b) to $H_2Ru_2(CO)_5$(ⁱPrNC(H)(Me)CH$_2$NⁱPr) (3b) and $Ru_2(CO)_6$(ⁱPrNC(H)(Me)CH$_2$NⁱPr) (4b). About 1 mmol of $Ru_2(CO)_6$(ⁱPr-DAB{H,Me}) (**1b**) was prepared in situ starting from 430 mg of $Ru_3(CO)_{12}$ (0.66 mmol) and 215 mg of ⁱPr-DAB{H,Me} (1.4 mmol).[10] Subsequently hydrogen was bubbled through the solution at 90 °C while the reaction was monitored by means of IR spectroscopy. After about 6 h IR spectroscopy indicated that only $H_2Ru_2(CO)_5$(ⁱPrNC(H)(Me)CH$_2$NⁱPr) (**3b**) and $Ru_2(CO)_6$(ⁱPrNC(H)(Me)CH$_2$NⁱPr) (**4b**) were present in solution. The reaction mixture was cooled to room temperature and subsequently brought upon a column for purification. Elution with ligroin afforded a pale yellow fraction containing both **3b** and **4b**. However, after evaporation of the solvent only $Ru_2(CO)_6$(ⁱPrNC(H)(Me)CH$_2$NⁱPr) (**4b**) was obtained in about 40% yield (based on $Ru_3(CO)_{12}$).

6. Monitoring the Reactions of $H_2Ru_2(CO)_5$(ⁱPr-DAB) (2a) with D_2 at 60 °C and of $D_2Ru_2(CO)_5$(ⁱPr-DAB) (2a′) with H_2 at 60 °C. (a) At 1 bar of H_2/D_2. A heptane solution (40 mL) of **2a** was prepared according literature procedures, starting from 300 mg of **1a**.[7] Subsequently the reaction mixture was evaporated to dryness and the residue was extracted with 40 mL of hexane. The extract was then stirred under 1 atm of deuterium at a temperature of 60 °C and analyzed by means of ^{1}H-NMR spectroscopy after 1, 2, and 4 h, respectively. Subsequently the deuterium atmosphere was replaced by an atmosphere of hydrogen and again the mixture was analyzed by means of ^{1}H-NMR spectroscopy after 1, 2, and 4 h, respectively. The NMR data indicated that treatment of **2a** with D_2 under these conditions led to a conversion to **2a′**, which reconverted to **2a** upon treatment with H_2. The bridging hydride/deuteride was found to exchange much more rapidly than the terminal one.

(b) High-Pressure Experiments. $Ru_2(CO)_6$(ⁱPr-DAB) (**1a**) (300 mg) was converted to $H_2Ru_2(CO)_5$(ⁱPr-DAB) (**2a**)[7] and subsequently evaporated to dryness. The residue was then extracted with 1.5 mL of C_6D_6, syringed into the sapphire HP-NMR tube, and pressurized with 20 bar of deuterium for 30 min. The tube was placed into the NMR spectrometer of which the sample space had been preheated to 323 K, and the reaction was monitored by ^{1}H-NMR spectroscopy in regular intervals. The resulting

(8) Staal, L. H.; Polm, L. H.; Vrieze, K.; Ploeger, F.; Stam, C. H. *Inorg. Chem.* **1981**, *20*, 3590.
(9) Kliegman, J. M.; Barnes, R. K. *J. Org. Chem.* **1970**, *35*, 3140.
(10) Staal, L. H.; Polm, L. H.; Balk, R. W.; Koten van, G.; Vrieze, K.; Brouwers, A. M. F. *Inorg. Chem.* **1980**, *19*, 3343.
(11) Roe, D. C. *J. Magn. Reson.* **1985**, *63*, 388.
(12) Especially the first fraction is extremely weakly colored.
(13) Both fractions were substantially contaminated with each other due to the poor separation of the fractions during column chromatography. In order to obtain **3a** and **4a** in a pure form it was found to be necessary to apply additional column chromatography on both fractions for at least two more times. Alternatively **3a** may be purified by a selective crystallization since **3a** precipitates much faster than **4a**.

Table I. Crystallographic Data for $H_2Ru_2(CO)_5(^iPrNCH_2CH_2N^iPr)$ (3a) and $Ru_2(CO)_6(^iPrNCH_2CH_2N^iPr)$ (4a)

	3a	4a
	Crystal Data	
formula	$C_{13}H_{20}N_2O_5Ru_2$	$C_{14}H_{18}N_2O_6Ru_2$
M_r	486.45	512.45
cryst system	monoclinic	orthorhombic
space group	$P2_1/c$ (No. 14)	$P2_1ab$ (No. 29)
a, Å	9.832 (1)	13.741 (1)
b, Å	16.164 (2)	14.496 (1)
c, Å	12.079 (2)	19.271 (1)
β, deg	109.72 (1)	-
V, Å^3	1807.1 (1)	3838.6 (4)
D_{calc}	1.788	1.773
Z	4	8
$F(000)$	960	2016
μ, cm^{-1}	16.6	15.7
cryst size, mm	0.11 × 0.08 × 0.38	0.40 × 0.40 × 0.40
	Data Collection	
temp, K	295	295
radiation (λ, Å)	Mo Kα (Zr) (0.71073)	Mo Kα (Zr) (0.71073)
$\theta_{min}/\theta_{max}$, deg	1.0, 27.5	1.0, 3.0
scan type	$\omega/2\theta$	$\omega/2\theta$
$\Delta\omega$, deg	0.80 + 0.35 tan θ	0.60 + 0.35 tan θ
hor and vert aperture, mm	3.00, 6.00	3.00, 6.00
ref reflns	0 0 2, 1 -1 0	4 7 10, -4 7 -10
dataset	-12/12, -20/0, 0/15	0/19, 0/20, 0/27
tot. data	4489	6171
unique data	4137	5797
obsd data [$I > 2.5\sigma(I)$]	2535	4251
	Refinement	
N_{ref}, N_{par}	2535, 262	4249, 460
R, R_w, S	0.039, 0.036, 1.87	0.034, 0.034, 1.57
weighting scheme	$1/\sigma^2(F)$	$1/\sigma^2(F)$
max and av shift/error	0.01, 0.001	0.18, 0.01
max/min resid density, e Å^{-3}	-0.56, 0.56	-0.59, 0.59

NMR data showed an H/D exchange similar to the one observed at atmospheric pressure.

7. Synthesis of $Ru_2(CO)_5(PPh_3)(^iPrNC(H)(X)CH_2N^iPr)$ (X = H (5a); X = Me (5b)). An amount of 0.33 mmol of $Ru_2(CO)_6(^iPrNC(H)(X)CH_2N^iPr)$ (X = H (4a); X = Me (4b)) was dissolved in 30 mL of toluene, and the solution was cooled to -60 °C by means of an ethanol/CO_2 bath. Subsequently the solution was treated with small portions of Me_3NO in CH_2Cl_2 until IR spectroscopy indicated that the starting complex 4 was no longer present. An amount of 130 mg of PPh_3 (0.5 mmol) was then added to the reaction mixture, which was then slowly allowed to reach room temperature. Subsequently the reaction mixture was evaporated to dryness, dissolved in a minimum amount of CH_2Cl_2, and purified by means of column chromatography. Elution with ligroin/CH_2Cl_2 afforded a pale yellow fraction, which after evaporation of the solvent afforded $Ru_2(CO)_5(PPh_3)(^iPrNC(H)(X)CH_2N^iPr)$ (X = H (5a); X = Me (5b)) in more than 80% yield.

8. Attempted H/D Exchange for $H_2Ru_2(CO)_5(^iPrNCH_2CH_2N^iPr)$ (3a). An amount of 150 mg of $H_2Ru_2(CO)_5(^iPrNCH_2CH_2N^iPr)$ (3a) was dissolved in 40 mL of heptane, and the solution was stirred under an atmosphere of deuterium. The reaction mixture was analyzed by means of ^{1}H-NMR after 3 h at 90 °C and after 3 h at 100 °C. The NMR spectra showed no changes in the proton intensities of the two hydrides and the hydrogenated DAB ligand, and only a partial conversion to $Ru_2(CO)_6(^iPrNCH_2CH_2N^iPr)$ (4a) was observed.

9. X-ray Structure Determinations of $H_2Ru_2(CO)_5(^iPrNCH_2CH_2N^iPr)$ (3a) and $Ru_2(CO)_6(^iPrNCH_2CH_2N^iPr)$ (4a). X-ray data were collected on an Enraf-Nonius CAD4 diffractometer for crystals mounted on top of a glass fiber. Crystal data and numerical details of the structure determinations are given in Table I. Unit cell parameters and their standard deviations were derived from the SET4 setting angles of 25 reflections in the range 11° < θ < 18° (3a) and 15° < θ < 18° (4a), respectively. The space groups consistent with the observed systematic absences are $P2_1/c$ and $P2_1ab$ or $Pmab$. The space group $P2_1ab$ (nonstandard setting of $Pca2_1$) was chosen on the basis of the successful structure determination in that space group. Data were collected for a small linear decay as indicated by three reference reflections and Lorentz and polarization effects but not for absorption. The structures were solved with the PATT option of SHELXS86[14] and refined on F by full-matrix least-squares with SHELX76.[15] All non-hydrogen atoms were refined with anisotropic thermal parameters. Hydrogen atoms were introduced on calculated positions (4a) or located from a difference map (3a) and their positions refined. The absolute structure of 4a was checked. Two low-order reflections were left out of the final refinement cycles for 4a.

Neutral scattering factors were obtained from Cromer and Mann[16] and corrected for anomalous dispersion.[17] The programs PLATON and PLUTON of the EUCLID package[18] were used for the geometrical calculations and molecular graphics. All calculations were done on a micro-VAX cluster.

Scheme I. Observed Reaction Sequence for the Hydrogenation of Complexes 2 to 3-5 and the Separate Conversion of 4 to 5 via Reaction with Me_2NO

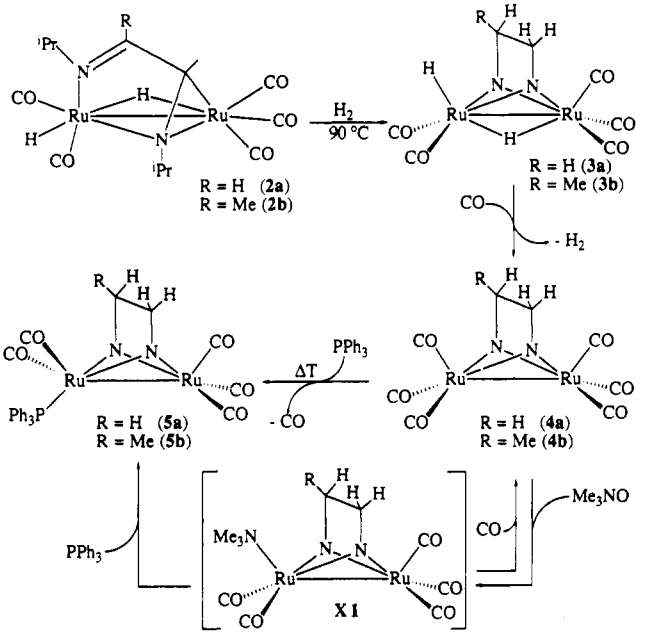

Results and Discussion

Synthesis and Structures of the New Complexes. The novel complexes $H_2Ru_2(CO)_5(^iPrNCH_2CH_2N^iPr)$ (3a) and $Ru_2(CO)_6(^iPrNCH_2CH_2N^iPr)$ (4a) were obtained by treatment of $H_2Ru_2(CO)_5(^iPr\text{-}DAB)$ (2a) with hydrogen at 90 °C in good yields. Complex 3a could thermally be converted to 4a at 80 °C. For ^{i}Pr-DAB{H,Me} the dihydride derivative could be detected spectroscopically, but only $Ru_2(CO)_6(^iPrNC(H)(Me)CH_2N^iPr)$ (4b) was isolated. The observed reaction sequence is outlined in Scheme I. Complexes 4a and 4b could be converted to $Ru_2(CO)_5(PPh_3)(^iPrNC(H)(X)CH_2N^iPr)$ (X = H (5a); X = Me (5b)) (Scheme I). The structures of complexes 3a and 4a have been confirmed by means of X-ray crystallography. The proposed structures of complexes 5a,b are based on spectroscopic data as will be described below. In the following we will first discuss the structural and spectroscopic aspects of the relevant complexes and subsequently

(14) Sheldrick, G. M. SHELXS86, Program for crystal structure determination. University of Göttingen, Germany, 1986.
(15) Sheldrick, G. M. SHELX76, Program for crystal structure determination. University of Cambridge, England, 1976.
(16) Cromer, D. T.; Mann, J. B. *Acta Crystallogr., Sect. A* **1968**, *A24*, 321.
(17) Cromer, D. T.; Liberman, D. *J. Chem. Phys.* **1970**, *53*, 1891.
(18) Spek, A. L. The EUCLID package. In *Computional Crystallography*; Sayre, D., Ed.; Clarendon Press: Oxford, U.K. 1982; p 528.

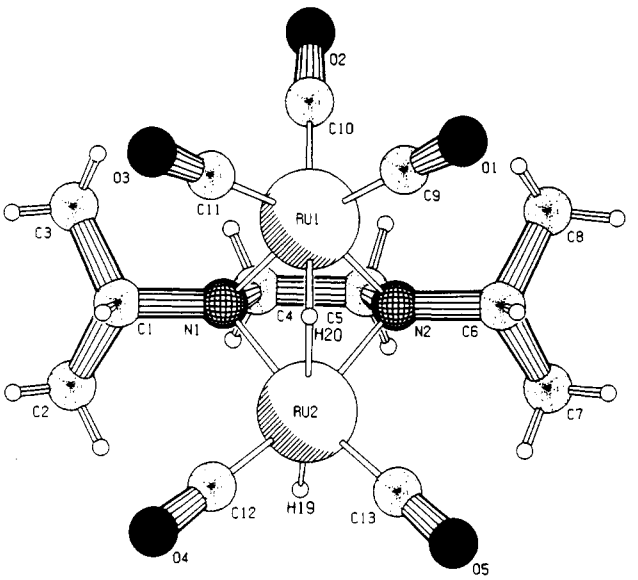

Figure 2. Molecular structure of $H_2Ru_2(CO)_5(^iPrNCH_2CH_2N^iPr)$ (**3a**).

Table II. Fractional Coordinates and Equivalent Isotropic Parameters of the Non-Hydrogen Atoms of $H_2Ru_2(CO)_5(^iPrNCH_2CH_2N^iPr)$ (3a) (with Esd's in Parentheses)

atom	*x*	*y*	*z*	*U*(eq),[a] Å^2
Ru(1)	0.24816 (5)	0.11829 (3)	0.18957 (4)	0.0329 (2)
Ru(2)	0.24440 (6)	0.27415 (3)	0.26747 (4)	0.0375 (2)
O(1)	0.4806 (6)	0.0803 (3)	0.0810 (5)	0.074 (2)
O(2)	0.2498 (6)	−0.0600 (3)	0.2770 (5)	0.0667 (19)
O(3)	0.0090 (6)	0.0884 (3)	−0.0445 (4)	0.070 (2)
O(4)	0.0110 (7)	0.3913 (4)	0.1311 (6)	0.087 (3)
O(5)	0.4655 (7)	0.4017 (4)	0.2666 (6)	0.094 (3)
N(1)	0.1174 (5)	0.1710 (3)	0.2785 (4)	0.0371 (17)
N(2)	0.3793 (5)	0.1736 (3)	0.3487 (4)	0.0381 (17)
C(1)	−0.0415 (7)	0.1714 (4)	0.2262 (6)	0.046 (2)
C(2)	−0.1112 (9)	0.2287 (6)	0.2926 (8)	0.067 (3)
C(3)	−0.1083 (10)	0.0858 (6)	0.2136 (9)	0.071 (3)
C(4)	0.1692 (8)	0.1400 (5)	0.4008 (6)	0.046 (3)
C(5)	0.3333 (8)	0.1422 (4)	0.4449 (6)	0.046 (3)
C(6)	0.5389 (7)	0.1766 (5)	0.3788 (6)	0.049 (3)
C(7)	0.6101 (10)	0.2350 (6)	0.4819 (8)	0.073 (3)
C(8)	0.6110 (10)	0.0916 (6)	0.4056 (8)	0.068 (3)
C(9)	0.3924 (8)	0.0942 (4)	0.1200 (6)	0.047 (3)
C(10)	0.2486 (7)	0.0054 (4)	0.2460 (5)	0.042 (2)
C(11)	0.0985 (7)	0.0981 (4)	0.0418 (6)	0.043 (2)
C(12)	0.0996 (8)	0.3468 (4)	0.1846 (6)	0.049 (3)
C(13)	0.3808 (8)	0.3519 (4)	0.2658 (6)	0.056 (3)

[a] U(eq) = $^1/_3$ of the trace of the orthogonalized *U*.

deal with the hydrogenation reactions.

Molecular Structure of $H_2Ru_2(CO)_5(^iPrNCH_2CH_2N^iPr)$ (3a). A view of the molecular structure of complex **3a** is shown in Figure 2 together with the atomic numbering. Tables II–IV contain the fractional coordinates, bond lengths, and bond angles of the non-hydrogen atoms of **3a**, respectively.

The molecular structure of **3a** consists of a $Ru(CO)_3$ unit and a $Ru(CO)_2(H)$ unit that are bridged by a hydride ligand and two *N*-amido bridges and which are further linked by a Ru–Ru bond (2.6939 (8) Å). This value is relatively small for a Ru–Ru bond, which usually varies between 2.70 and 2.90 Å.[2,7,19-21] Although this short metal–metal distance was not expected, since bridging hydrides have a lengthening effect,[20] it appears that this effect is compensated by the shortening effect of the small bite angle of the nitrogen bridges of the reduced DAB ligand.[2,6]

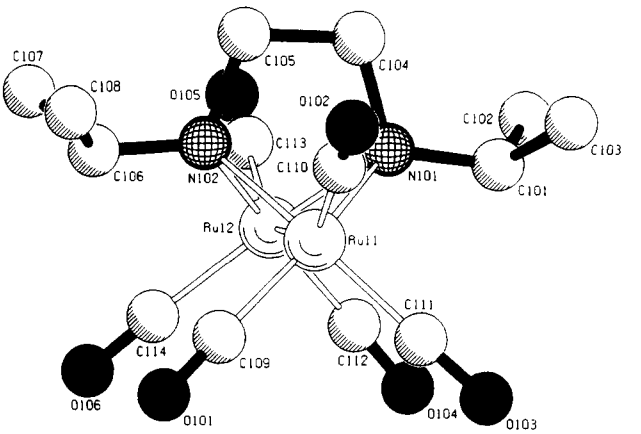

Figure 3. Molecular structure of one of the residue molecules of $Ru_2(CO)_6(^iPrNCH_2CH_2N^iPr)$ (**4a**).

The plane defined by C(1)N(1)C(4)C(5)N(2)C(6) is virtually flat (largest deviation: N(2) (0.015 Å)) and is oriented perpendicular to the metal–metal bond (89.8 (3)°). Although we are dealing with two metals that have a different coordination sphere, the hydrogenated DAB ligand is coordinated in the middle between these two metal centers (Ru(1)–N = 2.1155 Å (mean) and Ru(2)–N = 2.116 Å (mean)), indicating equivalent bond strengths between the nitrogen atoms and the two nonequivalent metal centers.

From the various Ru(1)–CO distances (Ru(1)–C(9) = 1.917 (8) Å, Ru(1)–C(10) = 1.947 (6) Å, Ru(1)–C(11) = 1.920 (7) Å) and C–O distances (C(9)–O(1) = 1.14 (1) Å, C(10)–O(2) = 1.120 (8) Å, C(11)–O(3) = 1.125 (9) Å) it appears that C(10)O(2) is less strongly coordinated to the metal center than C(9)O(1) and C(11)O(3), which might be due to the strong trans labilizing effect of the bridging hydride ligand.[22,23]

Molecular Structure of $Ru_2(CO)_6(^iPrNCH_2CH_2N^iPr)$ (4a). The molecular geometry of complex **4a** together with the atomic numbering is shown in Figure 3. Tables V–VII contain the fractional coordinates, bond lengths, and bond angles of the non-hydrogen atoms of **4a**, respectively.

The crystals of **4a** contain two independent molecules within the unit cell. Since these two molecules possess only slightly different geometries, only one of the independent molecules will be discussed. The molecular structure consists of two $Ru(CO)_3$ units that are bridged by a hydrogenated DAB ligand. The molecule has a Ru–Ru bond with a short bond length of 2.5745 (7) Å.[2,19,20] The distance is also substantially shorter than the one observed for **3a** (vide supra), which is understandable since the shortening effect of the small bite of the diamido ligand[2,6] is not compensated by a bridging hydride. The bite angles (N(101)Ru(11)N(102) = 70.9 (2)°, N(101)Ru(12)N(102) = 70.76° (20)) are as expected for dinitrogen-bridged species.[2,5,6,24]

(19) Bennett, M. A.; Bruce, M. I.; Matheson, T. W. In *Comprehensive Organometallic Chemistry*; Wilkinson, G., Stone, F. G. A., Abel, E. W., Eds.; Pergamon Press: Oxford, U.K., 1982; Chapter 32.4, pp 821–841.
(20) Bruce, M. I. In *Comprehensive Organometallic Chemistry*; Wilkinson, G., Stone, F. G. A., Abel, E. W., Eds.; Pergamon Press: Oxford, U.K., 1982; Vol. IV, Chapter 32.5, p 846.
(21) Keijsper, J.; Abbel, G.; Koten van, G.; Polm, L. H.; Stam, C. H.; Vrieze, K. *Inorg. Chem.* **1984**, *23*, 2142.
(22) Zuhmdahl, S. S.; Drago, R. S. *J. Am. Chem. Soc.* **1968**, *90*, 6669.
(23) Huheey, J. E. In *Inorganic Chemistry*, 3rd ed.; Harper Collins Publishers: New York, 1983; pp 538–545.
(24) Dahl, L. F.; Costello, W. R.; King, R. B. *J. Am. Chem. Soc.* **1968**, *90*, 5422.

Table III. Bond Distances (Å) of the Hydride Atoms and the Non-Hydrogen Atoms of $H_2Ru_2(CO)_5(^iPrNCH_2CH_2N^iPr)$ (3a) (with Esd's in Parentheses)

Ru(1)–Ru(2)	2.6939 (8)	Ru–N(1)	2.113 (5)	Ru(1)–N(2)	2.118 (5)
Ru(1)–C(9)	1.917 (8)	Ru(1)–C(10)	1.947 (6)	Ru(1)–C(11)	1.920 (7)
Ru(2)–N(1)	2.114 (5)	Ru(2)–N(2)	2.118 (5)	Ru(2)–C(12)	1.856 (7)
Ru(2)–C(13)	1.843 (7)	O(1)–C(9)	1.14 (1)	O(2)–C(10)	1.120 (8)
O(3)–C(11)	1.125 (9)	O(4)–C(12)	1.146 (10)	O(5)–C(13)	1.156 (10)
N(1)–C(1)	1.474 (9)	N(1)–C(4)	1.478 (8)	N(2)–C(5)	1.472 (9)
N(2)–C(6)	1.487 (9)	C(1)–C(2)	1.530 (12)	C(1)–C(3)	1.517 (12)
C(4)–C(5)	1.519 (11)	C(6)–C(7)	1.531 (12)	C(6)–C(8)	1.530 (13)
Ru(1)–H(20)	1.61 (5)	Ru(2)–H(20)	1.82 (5)	Ru(2)–H(19)	1.63 (6)

Table IV. Bond Angles (deg) of the Hydride Atoms and the Non-Hydrogen Atoms of $H_2Ru_2(CO)_5(^iPrNCH_2CH_2N^iPr)$ (3a) (with Esd's in Parentheses)

Ru(2)–Ru(1)–N(1)	50.43 (13)	Ru(1)–C(10)–O(2)	178.8 (6)	N(2)–Ru(2)–C(13)	100.6 (3)
Ru(2)–Ru(1)–C(9)	116.3 (2)	Ru(2)–C(12)–O(4)	178.4 (7)	Ru(1)–N(1)–Ru(2)	79.18 (18)
Ru(2)–Ru(1)–C(11)	112.78 (20)	Ru(2)–Ru(1)–H(20)	41 (2)	Ru(1)–N(1)–C(4)	107.9 (4)
N(1)–Ru(1)–C(9)	166.4 (2)	N(2)–Ru(1)–H(20)	81 (2)	Ru(2)–N(1)–C(4)	108.6 (4)
N(1)–Ru(1)–C(11)	97.7 (2)	C(10)–Ru(1)–H(20)	180 (2)	Ru(1)–N(2)–Ru(2)	79.00 (16)
N(2)–Ru(1)–C(10)	98.6 (2)	Ru(1)–Ru(2)–H(20)	35.7 (16)	Ru(1)–N(2)–C(6)	120.3 (4)
C(9)–Ru(1)–C(10)	92.8 (3)	N(1)–Ru(2)–H(20)	77.8 (18)	Ru(2)–N(2)–C(6)	122.2 (4)
C(10)–Ru(1)–C(11)	94.4 (3)	N(2)–Ru(2)–H(20)	77.1 (17)	N(1)–C(1)–C(2)	112.0 (6)
Ru(1)–Ru(2)–N(2)	50.50 (13)	H(20)–Ru(2)–C(12)	97.2 (18)	C(2)–C(1)–C(3)	110.4 (7)
Ru(1)–Ru(2)–C(13)	122.6 (2)	H(20)–Ru(2)–H(19)	174 (2)	N(2)–C(5)–C(4)	107.7 (5)
N(1)–Ru(2)–C(12)	99.9 (3)	C(13)–Ru(2)–H(19)	87 (2)	N(2)–C(6)–C(8)	113.4 (7)
N(2)–Ru(2)–C(12)	169.0 (3)	Ru(2)–Ru(1)–N(2)	50.51 (13)	Ru(1)–C(9)–O(1)	178.4 (6)
C(12)–Ru(2)–C(13)	89.5 (3)	Ru(2)–Ru(1)–C(10)	138.83 (18)	Ru(1)–C(11)–O(3)	178.0 (6)
Ru(1)–N(1)–C(1)	121.5 (4)	N(1)–Ru(1)–N(2)	69.93 (19)	Ru(2)–C(13)–O(5)	178.5 (7)
Ru(2)–N(1)–C(1)	122.2 (4)	N(1)–Ru(1)–C(10)	97.5 (2)	N(1)–Ru(1)–H(20)	82 (2)
C(1)–N(1)–C(4)	112.8 (5)	N(2)–Ru(1)–C(9)	99.8 (3)	C(9)–Ru(1)–H(20)	88 (2)
Ru(1)–N(2)–C(5)	108.4 (4)	N(2)–Ru(1)–C(11)	163.1 (2)	C(11)–Ru(1)–H(20)	86 (2)
Ru(2)–N(2)–C(5)	108.6 (4)	C(9)–Ru(1)–C(11)	90.4 (3)	Ru(1)–Ru(2)–H(19)	138.4 (18)
C(5)–N(2)–C(6)	113.5 (5)	Ru(1)–Ru(2)–N(1)	50.39 (13)	N(1)–Ru(2)–H(19)	95.8 (19)
N(1)–C(1)–C(3)	113.5 (6)	Ru(1)–Ru(2)–C(12)	120.1 (2)	N(2)–Ru(2)–H(19)	99.7 (19)
N(1)–C(4)–C(5)	108.0 (6)	N(1)–Ru(2)–N(2)	69.91 (19)	H(20)–Ru(2)–C(13)	98.9 (18)
N(2)–C(6)–C(7)	112.0 (6)	N(1)–Ru(2)–C(13)	170.4 (3)	C(12)–Ru(2)–H(19)	84.9 (20)
C(7)–C(6)–C(8)	109.2 (7)				

As in the case of **3a** the plane defined by C(101)N(101)C(104)C(105)N(102)C(106) is virtually flat with the largest deviation from the plane being 0.01 Å. This plane is oriented perpendicular to the metal–metal bond (89.9 (3)°). The four metal–nitrogen bonds are equivalent, indicating that the hydrogenated DAB ligand is positioned in the middle between the two metal centers. The nature of these metal–nitrogen bonds has been subject of a separate study, from which it was concluded that the main source of the M–N bonding is π in nature, while σ contributions are less important.[25]

IR Spectroscopy and Analyses. The IR spectroscopic data of the ν(CO) region are listed in Table VIII together with the results of the elemental analyses. All complexes show a characteristic absorption pattern. From the positions of the absorption maxima it can be concluded that all complexes only contain terminally coordinated carbonyls.

NMR Spectroscopy. The ^{1}H-NMR and ^{13}C-NMR data have been listed in Tables IX and X, respectively. Since the two isopropyl groups are equivalent, both the ^{1}H-NMR spectrum and the ^{13}C-NMR spectrum of **3a** (Figure 4A) show only two signals for the four ^{i}PrMe groups. In benzene the ^{1}H-NMR spectrum shows only one multiplet for the four H atoms of the C_2H_4 fragment and the two ^{i}PrCH atoms. However in CD_2Cl_2 three sets of signals have been observed, each with a relative intensity of two protons. In this case the four H atoms of the C_2H_4 moiety appear as two sets of double doublets, each broadened as a result of second-order coupling effects. The ^{1}H-NMR spectrum further shows two doublets in the metal–hydride region. Attempts to assign the signals to the bridging hydride or the terminal hydride respectively using NOE-difference NMR techniques failed, despite the relative short distance between the terminal hydride and the H atoms of the C_2H_4 moiety, as was indicated for the solid state (2.77 and 2.84 Å, respectively).

The highly symmetrical geometry of **4a** is evidenced both by the ^{1}H-NMR and the ^{13}C-NMR spectra. The four ^{i}PrMe groups, the two ^{i}PrCH groups, and the C_2H_4 moiety give each rise to one signal, both in the ^{1}H-NMR and in the ^{13}C-NMR spectra. The carbonyl region of the ^{13}C-NMR spectrum contains two signals with an intensity of about 1:2, which shows that carbonyls a and b are equivalent as well as the carbonyls c–f (Figure 4B).

In the ^{13}C-NMR spectra of the deuterated **3a′** and **4a′** only a very broad and weak signal was observed for the carbon atoms of the C_2 unit of the reduced DAB ligand, in contrast with the results obtained for the FeRu system,[6] in which the detection of a triplet indicated the presence of two equivalent CHD centers. This phenomenon probably arises from the poor selectivity of the reduction process for the system reported here (vide infra), resulting in the presence of C_2D_4, C_2HD_3, and $C_2H_2D_2$ moieties in the products.

In order from **4a** to **4b** the symmetry of the complex is reduced by the presence of a methyl group on the hydrogenated DAB ligand. The ^{1}H-NMR spectrum and its assignment are analogous to the heteronuclear analogue $FeRu(CO)_6(^iPrNC(H)(Me)CH_2N^iPr$.[6] The signal belonging to H_3 is observed as a multiplet together with the septet of one of the ^{i}PrCH atoms. H_1 and H_2 both give rise to a set of doublets of doublets as a result of a coupling with each other[26] and with H_3. The assignment of H_1 and H_2

(25) Casarin, M.; Guline, A.; Kraakman, M. J. A.; Rizzi, G. A.; Vittadini, A.; Vrieze, K. *Inorg. Chem.* **1991**, *30*, 1906.

(26) As found for the heteronuclear analogue,[6] the sign of the coupling is probably negative since a value of −10.8 Hz would be a typical value for a coupling between two geminal protons. However no attempts were made to confirm this assumption.

Table V. Fractional Coordinates and Equivalent Isotropic Parameters of the Non-Hydrogen Atoms of Both Residue Molecules of $Ru_2(CO)_6$(ⁱPrNCH$_2$CH$_2$NⁱPr) (4a) (with Esd's in Parentheses)

atom	x	y	z	U(eq),[a] Å²
Ru(11)	0	0.13132 (3)	0.12085 (2)	0.0403 (1)
Ru(12)	−0.05913 (5)	−0.03719 (3)	0.12254 (3)	0.0416 (2)
O(101)	0.2141 (5)	0.1248 (5)	0.1606 (4)	0.104 (3)
O(102)	−0.0308 (9)	0.3288 (3)	0.1705 (3)	0.127 (4)
O(103)	0.0583 (6)	0.1806 (4)	−0.0272 (3)	0.093 (3)
O(104)	−0.0288 (7)	−0.1007 (4)	−0.0256 (3)	0.101 (3)
O(105)	−0.2126 (5)	−0.1801 (5)	0.1644 (4)	0.098 (3)
O(106)	0.1166 (5)	−0.1523 (5)	0.1666 (4)	0.095 (3)
N(101)	−0.1401 (4)	0.0820 (3)	0.0974 (3)	0.0460 (17)
N(102)	−0.0536 (4)	0.0561 (3)	0.2065 (2)	0.0407 (14)
C(101)	−0.1844 (6)	0.0939 (5)	0.0278 (4)	0.058 (3)
C(102)	−0.2677 (8)	0.0272 (7)	0.0147 (5)	0.087 (4)
C(103)	−0.2175 (8)	0.1930 (6)	0.0145 (5)	0.085 (4)
C(104)	−0.2071 (6)	0.1031 (6)	0.1552 (4)	0.059 (3)
C(105)	−0.1526 (5)	0.0884 (5)	0.2236 (3)	0.052 (3)
C(106)	0.0072 (6)	0.0375 (4)	0.2689 (3)	0.054 (2)
C(107)	−0.0373 (9)	−0.0357 (5)	0.3154 (4)	0.073 (3)
C(108)	0.0269 (8)	0.1253 (6)	0.3108 (4)	0.084 (4)
C(109)	0.1345 (7)	0.1273 (6)	0.1463 (5)	0.065 (3)
C(110)	−0.0216 (7)	0.2569 (5)	0.1525 (3)	0.067 (3)
C(111)	0.0375 (6)	0.1621 (5)	0.0291 (4)	0.058 (3)
C(112)	−0.0417 (7)	−0.0790 (4)	0.0316 (4)	0.067 (3)
C(113)	−0.1568 (6)	−0.1255 (6)	0.1493 (4)	0.058 (3)
C(114)	0.0509 (7)	−0.1115 (5)	0.1515 (4)	0.062 (3)
Ru(21)	0.37316 (6)	−0.03624 (3)	0.37686 (3)	0.0400 (1)
Ru(22)	0.55964 (6)	−0.04168 (3)	0.37456 (3)	0.0416 (2)
O(201)	0.3264 (5)	0.0423 (5)	0.5191 (3)	0.085 (3)
O(202)	0.1827 (5)	−0.1357 (5)	0.3449 (4)	0.101 (3)
O(203)	0.3220 (6)	0.1506 (4)	0.3132 (4)	0.102 (3)
O(204)	0.6246 (5)	0.1362 (4)	0.3053 (5)	0.101 (3)
O(205)	0.7447 (5)	−0.1512 (4)	0.3414 (4)	0.095 (3)
O(206)	0.6168 (6)	0.0356 (5)	0.5155 (4)	0.094 (3)
N(201)	0.4634 (4)	−0.0843 (3)	0.2960 (2)	0.0380 (12)
N(202)	0.4650 (5)	−0.1419 (3)	0.4150 (2)	0.0443 (16)
C(201)	0.4632 (7)	−0.0424 (4)	0.2260 (3)	0.0553 (19)
C(202)	0.5564 (9)	−0.0664 (7)	0.1862 (5)	0.085 (4)
C(203)	0.3718 (8)	−0.0654 (7)	0.1848 (4)	0.077 (3)
C(204)	0.4603 (6)	−0.1875 (3)	0.2936 (3)	0.0457 (19)
C(205)	0.4609 (6)	−0.2229 (4)	0.3686 (3)	0.0523 (19)
C(206)	0.4665 (8)	−0.1698 (4)	0.4890 (3)	0.064 (3)
C(207)	0.5552 (11)	−0.2264 (8)	0.5087 (5)	0.107 (5)
C(208)	0.3692 (11)	−0.2157 (7)	0.5112 (5)	0.109 (5)
C(209)	0.3417 (5)	0.0131 (6)	0.4651 (4)	0.056 (3)
C(210)	0.2535 (6)	−0.0986 (6)	0.3568 (4)	0.059 (3)
C(211)	0.3399 (6)	0.0799 (6)	0.3346 (4)	0.063 (3)
C(212)	0.6022 (6)	0.0699 (6)	0.3311 (5)	0.061 (3)
C(213)	0.6764 (6)	−0.1118 (6)	0.3536 (5)	0.062 (3)
C(214)	0.5981 (6)	0.0067 (6)	0.4618 (5)	0.062 (3)

[a] U(eq) = 1/3 of the trace of the orthogonalized U.

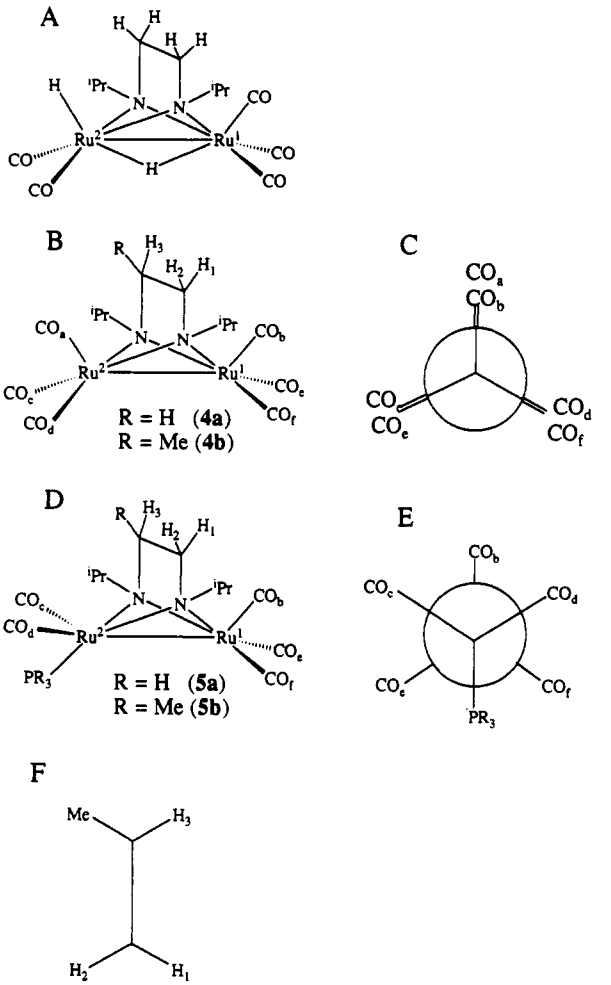

Figure 4. Structures of complexes **3a** (A) and **4a,b** (B and C) and proposed structures for complexes **5a,b** (D and E), including the assignment of the carbonyl ligands and the $CH_2C(H)(R)$ moieties (F).

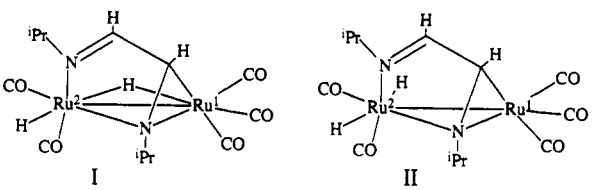

Figure 5. Possible structures for complex **2a**.

can be made on basis of the Karplus equation, which predicts the coupling between H_3 and H_1 to be larger than the coupling between H_3 and H_2 (dihedral angles of about 0 and 120°, respectively). In the ^{13}C-NMR spectrum the asymmetry is also clear, since all ⁱPrMe groups and both ⁱPrCH groups now appear as separate signals. The two carbon atoms of the $CH_2C(H)(Me)$ moiety have been distinguished by using an APT pulse sequence.

The ^{1}H-NMR spectrum of **5a** shows two doublets for the four ⁱPrMe groups, indicating the presence of two equivalent ⁱPr groups that give rise to two signals for the diastereotopic Me groups. The two sides of the C_2H_4 moiety have now become inequivalent due to the introduction of a phosphine ligand on one of the ruthenium atoms. The C_2H_4 moiety therefore gives rise to two sets of signals at 2.37 and 2.70 ppm, respectively, which is analogous to the pattern observed for **3a** (vide supra).

The carbonyl region of the ^{13}C-NMR spectrum of **5a** shows a doublet at 189.3 ppm (18.7 Hz), a singlet at 202.9 ppm, and a doublet at 207.1 ppm (4.4 Hz) with a relative

Table VI. Bond Distances (Å) of the Non-Hydrogen Atoms of One of the Residue Molecules of $Ru_2(CO)_6$(ⁱPrNCH$_2$CH$_2$NⁱPr) (4a) (with Esd's in Parentheses)

Ru(11)–Ru(12)	2.5745 (7)	Ru(11)–N(101)	2.103 (5)	Ru(11)–N(102)	2.111 (4)
Ru(11)–C(109)	1.913 (10)	Ru(11)–C(110)	1.943 (7)	Ru(11)–C(111)	1.895 (8)
Ru(12)–N(101)	2.111 (5)	Ru(12)–N(102)	2.110 (4)	Ru(12)–C(112)	1.870 (8)
Ru(12)–C(113)	1.925 (8)	Ru(12)–C(114)	1.938 (9)	O(101)–C(109)	1.129 (12)
O(102)–C(110)	1.106 (9)	O(103)–C(111)	1.154 (10)	O(104)–C(112)	1.16 (1)
O(105)–C(113)	1.140 (11)	O(106)–C(114)	1.118 (11)	N(101)–C(101)	1.483 (10)
N(101)–C(104)	1.477 (10)	N(102)–C(105)	1.476 (9)	N(102)–C(106)	1.489 (8)
C(101)–C(102)	1.519 (13)	C(101)–C(103)	1.528 (12)	C(104)–C(105)	1.531 (10)
C(106)–C(107)	1.518 (11)	C(106)–C(108)	1.531 (10)		

Table VII. Bond Angles (deg) of the Non-Hydrogen Atoms of One of the Residue Molecules of $Ru_2(CO)_6(^iPrNCH_2CH_2N^iPr)$ (4a) (with Esd's in Parentheses)

Ru(12)-Ru(11)-N(101)	52.50 (12)	Ru(12)-Ru(11)-N(102)	52.40 (12)
Ru(12)-Ru(11)-C(109)	105.8 (3)	Ru(12)-Ru(11)-C(110)	146.8 (3)
Ru(12)-Ru(11)-C(111)	108.7 (2)	N(101)-Ru(11)-N(102)	70.9 (2)
N(101)-Ru(11)-C(109)	158.3 (3)	N(101)-Ru(11)-C(110)	104.3 (3)
N(101)-Ru(11)-C(111)	97.4 (3)	N(102)-Ru(11)-C(109)	96.9 (3)
N(102)-Ru(11)-C(110)	100.7 (2)	N(102)-Ru(11)-C(111)	161.1 (3)
C(109)-Ru(11)-C(110)	95.5 (4)	C(109)-Ru(11)-C(111)	89.1 (4)
C(110)-Ru(11)-C(111)	96.5 (3)	Ru(11)-Ru(12)-N(101)	52.19 (14)
Ru(11)-Ru(12)-N(102)	52.43 (12)	Ru(11)-Ru(12)-C(112)	104.8 (2)
Ru(11)-Ru(12)-C(113)	148.7 (3)	Ru(11)-Ru(12)-C(114)	106.5 (2)
N(101)-Ru(12)-N(102)	70.76 (20)	N(101)-Ru(12)-C(112)	96.8 (3)
N(101)-Ru(12)-C(113)	103.8 (3)	N(101)-Ru(12)-C(114)	158.7 (3)
N(102)-Ru(12)-C(112)	157.2 (2)	N(102)-Ru(12)-C(113)	104.2 (3)
N(102)-Ru(12)-C(114)	96.2 (3)	C(112)-Ru(12)-C(113)	97.2 (3)
C(112)-Ru(12)-C(114)	89.4 (3)	C(113)-Ru(12)-C(114)	95.6 (3)
Ru(11)-N(101)-Ru(12)	75.31 (18)	Ru(11)-N(101)-C(101)	122.0 (4)
Ru(11)-N(101)-C(104)	109.8 (4)	Ru(12)-N(101)-C(101)	121.3 (4)
Ru(12)-N(101)-C(104)	109.0 (4)	C(101)-N(101)-C(104)	113.7 (6)
Ru(11)-N(102)-Ru(12)	75.17 (13)	Ru(11)-N(102)-C(105)	109.4 (3)
Ru(11)-N(102)-C(106)	122.0 (4)	Ru(12)-N(102)-C(105)	110.0 (4)
Ru(12)-N(102)-C(106)	121.6 (4)	C(105)-N(102)-C(106)	113.2 (4)
N(101)-C(101)-C(102)	112.7 (6)	N(101)-C(101)-C(103)	112.5 (6)
C(102)-C(101)-C(103)	110.2 (8)	N(101)-C(104)-C(105)	108.4 (6)
N(102)-C(105)-C(104)	107.6 (5)	N(102)-C(106)-C(107)	112.2 (7)
N(102)-C(106)-C(108)	112.0 (5)	C(107)-C(106)-C(108)	109.9 (6)
Ru(11)-C(109)-O(101)	179.3 (9)	Ru(11)-C(110)-O(102)	177.8 (10)
Ru(11)-C(111)-O(103)	178.5 (8)	Ru(12)-C(112)-O(104)	176.6 (6)
Ru(12)-C(113)-O(105)	177.7 (8)	Ru(12)-C(114)-O(106)	177.3 (8)

Table VIII. IR Spectroscopic Data and Elemental Analyses for the Complexes 2b, 3a,b, 4a,b, and 5a,b and Intermediate X1

		elemental anal.: obsd, % (calcd, %)		
complex	IR: ν(C≡O), cm^{-1}	C	H	N
2b[a]	2073 (s), 2027 (vs), 1997 (vs, br), 1959 (vs)	not isolated		
3a[b]	2092 (m), 2020 (vs), 1953 (s)	32.25 (32.10)	3.98 (4.14)	5.75 (5.76)
3b[a]	2091 (m), 2023 (vs), 1958 (s)	not isolated		
4a[b]	2070 (m), 2039 (s), 1987 (vs), 1981 (vs), 1972 (m)	33.12 (32.81)	3.53 (3.53)	5.24 (5.47)
4b[b]	2071 (m), 2041 (s), 1987 (vs), 1981 (vs), 1972 (m)	34.33 (34.22)	3.81 (3.83)	5.16 (5.32)
5a[b]	2049 (s), 1986 (vs), 1974 (s), 1963 (s), 1924 (m)	50.30 (49.86)	4.61 (4.45)	3.67 (3.75)
5b[c]	2048 (s), 1982 (vs), 1972 (s), 1958 (s), 1920 (m)	50.61 (50.52)	4.64 (4.71)	3.75 (3.68)
X1[d,e]	2044 (s), 1955 (vs, br), 1871 (s)	not isolated		

[a] Heptane solution. [b] Hexane solution. [c] Hexane/CH_2Cl_2 (9/1). [d] Toluene solution. [e] Spectra obtained for ^{i}Pr-DAB{H,H} and ^{i}Pr-DAB{H,Me} showed the same absorption maxima for intermediate **X1**.

intensity of 1:2:2. A similar pattern has been observed for the heteronuclear analogue $FeRu(CO)_5(PPh_3)(^iPrNCH_2CH_2N^iPr)$.[27] Analogous to this heteronuclear complex we assign the signals at 189.3 and 207.8 ppm to the carbonyl ligands of the $Ru(CO)_3$ unit. The relatively large phosphorus coupling on the signal at 189.3 ppm may be rationalized by a staggered conformation of the two ML_3 fragments, leading to a trans arrangement of one of the carbonyls of the unsubstituted $M(CO)_3$ fragment and the phosphorus atom (Figure 4D,E). Such a staggered conformation is also attractive from a steric point of view since the large phosphine ligand is now situated on the sterically least demanding site. The dihedral angles between the Ru(2)–P bond and the Ru(1)–CO bonds in the staggered description (Figure 4) are about 180 and 45°, respectively, and therefore agree with the observed coupling constants. The carbonyls of the $Ru(CO)_2(PPh_3)$ fragment are coordinated in a cis position to the phosphine ligand, which explains that no phosphorus coupling on these carbonyl ligands is detected.

Table IX. ^{1}H-NMR Data (ppm) for the Complexes 3a, 4a,b, and 5a,b

3a[a]	2.97–2.68 (m, 4H, NCH_2CH_2N + ^{i}Pr-CH), 2.65–2.52 (m, 2H, NCH_2CH_2N), 1.18/0.84 (d/d, 6H/6H, 6.4 Hz/6.4 Hz, ^{i}Pr-CH_3), −7.91/−8.46 (d/d, 1H/1H, 15 Hz/15 Hz, Ru-H)
3a[b]	3.20/3.04 (m/m, 2H/2H, NCH_2CH_2N), 2.90 (sept, 2H, 6.5 Hz, ^{i}Pr-CH), 1.30/1.20 (d/d, 6H/6H, 6.5 Hz/6.5 Hz, ^{i}Pr-CH_3), −8.37/−8.79 (d/d, 1H/1H, 15 Hz/15 Hz, Ru-H)
4a[a]	3.17 (sept, 2H, 6.5 Hz, ^{i}Pr-CH), 2.54 (s, 4H, NCH_2CH_2N), 1.00 (d, 12H, 6.5 Hz, ^{i}Pr-CH_3)
4b[c,e]	3.73 (sept, 1H, 6.5 Hz, ^{i}Pr-CH), 3.14 (m, 2H, ^{i}Pr-CH + H_3), 2.80 (dd, 1H, 7.4 Hz/10.8 Hz, H_1), 2.13 (dd, 1H, 10.8 Hz/4.8 Hz, H_2), 0.94/0.98/1.07/1.12 (4 × d, 4 × 3H, 6.5 Hz, ^{i}Pr-CH_3), 0.70 (d, 3H, 6.1 Hz, CH_3)
5a[d]	7.62–7.31 (m, 15H, $P(-C_6H_5)_3$), 3.31 (sept, 2H, 6.5 Hz, ^{i}Pr-CH), 2.70/2.37 (m/m, 2H/2H, NCH_2CH_2N), 1.25/0.85 (d/d, 6H/6H, 6.5 Hz, ^{i}Pr-CH_3)
5b[d,e]	7.62–7.34 (m, 15H, $P(-C_6H_5)_3$), 3.53/3.25 (sept, 2H, 6.5 Hz, ^{i}Pr-CH), 2.60 (m, 2H, H_1 + H_3), 2.15 (dd, 1H, 9.4 Hz/3.7 Hz, H_2), 1.27/1.24/0.96/0.81 (4 × d, 4 × 3H, 6.5 Hz, ^{i}Pr-CH_3), 0.81 (d, 3H, 6.5 Hz, CH_3)

[a] C_6D_6 solution, 100.13 MHz. [b] CD_2Cl_2 solution, 250.13 MHz. [c] C_6D_6 solution, 250.13 MHz. [d] $CDCl_3$ solution, 100.13 MHz. [e] Assignment of the $CH_2C(H)(Me)$ moiety according to Figure 4.

Table X. ^{13}C-NMR Data (ppm) for the Complexes 3a, 4a,b, and 5a,b

3a[a]	22.9/24.7 (^{i}Pr-CH_3), 54.6 (NCH_2CH_2N), 63.8 (^{i}Pr-CH), 188.5 ($Ru(CO)_3$ (1×)), 192.5 ($Ru(CO)_2$ (2×)), 202.9 ($Ru(CO)_3$ (2×))
4a[a]	23.9 (^{i}Pr-CH_3), 54.2 (N-CH_2CH_2-N), 65.8 (^{i}Pr-CH), 189.7 (CO (2×)), 201.7 (CO (4×))
4b[b]	23.0/23.1/23.5/23.9 (^{i}Pr-CH_3), 29.4 (NC(CH_3)(H)CH_2N), 64.0 (N-C(CH_3)(H)-CH_2-N), 64.5 (N*C*(CH_3)(H)CH_2N), 65.6/67.5 (^{i}Pr-CH), 189.5/201.2/201.5 (CO)
5a[c,d]	23.3/24.9 (^{i}Pr-CH_3), 52.9/53.1 (NCH_2CH_2N), 63.8 (^{i}Pr-CH), 128.5 (d, 8.7 Hz, Ph-C^3/C^5), 130.0 (Ph-C^4), 133.5 (d, 11.5 Hz, Ph-C^2/C^6), 136.9 (d, 31.1 Hz, Ph-C^1), 189.3 (d, 18.7 Hz, $(CO)_b$), 202.9 (($CO)_c$ and $(CO)_d$)), 207.1 (d, 4.4 Hz, $(CO)_e$ and $(CO)_f$)
5b[c,d]	22.5/23.1/23.5/24.7 (^{i}Pr-CH_3), 30.8 (NC(CH_3)(H)CH_2N), 60.6 (d, 4.4 Hz, NC(CH_3)(H)*C*H_2N), 63.0 (br, N*C*(CH_3)(H)CH_2N), 63.8/65.3 (^{i}Pr-CH), 128.5 (d, 8.9 Hz, Ph-C^3/C^5), 129.9 (Ph-C^4), 133.6 (d, 11.4 Hz, Ph-C^2/C^6), 136.4 (d, 31.1 Hz, Ph-C^1), 190.1 (d, 19.5 Hz, $(CO)_b$), 202.4/203.0 (($CO)_c$ and $(CO)_d$)), 206.4/207.2 (d/d, 4.9 Hz/3.4 Hz, $(CO)_e$ and $(CO)_f$)

[a] C_6D_6 solution, 25.17 MHz. [b] C_6D_6 solution, 62.85 MHz. [c] $CDCl_3$ solution, 25.17 MHz. [e] Assignment of the carbonyls according Figure 4.

Complex **5b** is asymmetrical due to the presence of a Me group on the hydrogenated DAB ligand. All four ^{i}PrMe groups give separate signals, both in the ^{1}H-NMR and in the ^{13}C-NMR spectra. The signal of H_3 (Figure 4) now no longer coincides with one of the ^{i}PrCH atoms, and the latter are observed as two separate septets. The three protons of the $CH_2C(H)(Me)$ moiety now give rise to a multiplet at 2.60 ppm with a relative intensity of two H atoms and a doublet of doublets at 2.15 ppm. From the observed coupling constants it may be concluded that the latter belongs to H_2, and therefore the multiplet at 2.60 ppm belongs to H_1 and H_3.

The carbonyl region of the ^{13}C-NMR spectrum may, like suggested for **5a** (vide supra), again be explained by a staggered conformation of the $Ru(CO)_3$ fragment and the $Ru(CO)_2(PPh_3)$ fragment. However, due to the introduction of the methyl group the carbonyls c and d and the carbonyls e and f (Figure 4) are no longer equivalent, so that they are all observed separately.

(27) Kraakman, M. J. A.; Vrieze, K.; Numan, M.; Goubitz, K. *Inorg. Chim. Acta* **1992**, *202*, 197–210.

Scheme II. Proposed Mechanism for the Observed H/D Exchange of the Bridging Hydride in 2a

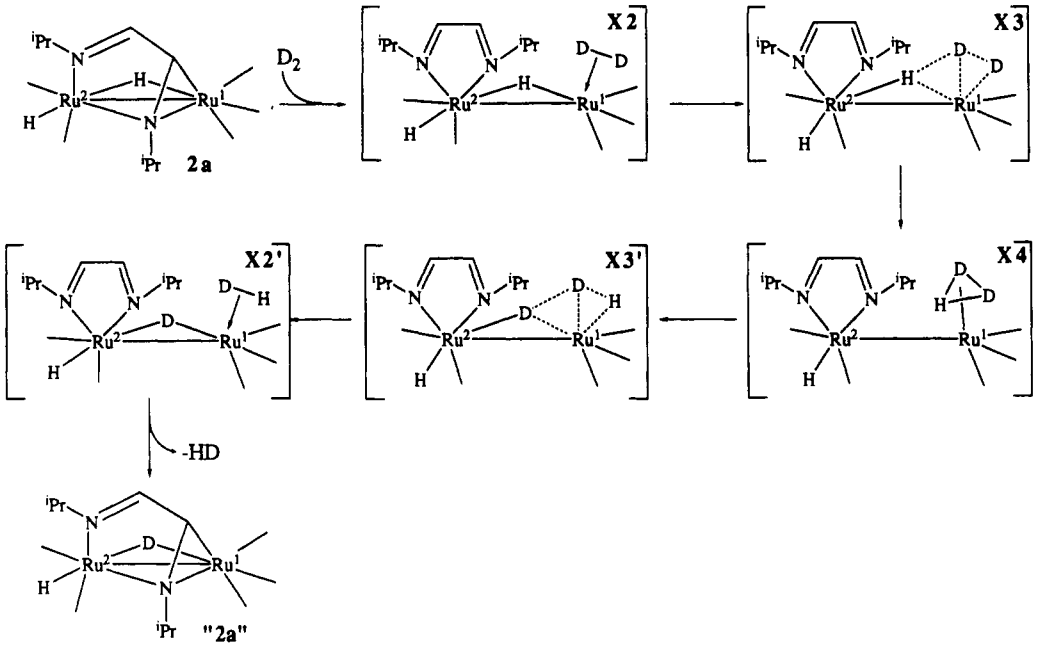

Since knowledge about the structure of the starting complex **2a** is important for a firm understanding of the mechanism of the hydrogenation reactions, and since we observed an interesting nonequivalence of the two hydride ligands in H/D exchange reactions (vide infra), we took a closer look at the structure of **2a**. It has been suggested, as based on the observed chemical shifts at −7.8 and −11.8 ppm, that both hydride ligands are terminally coordinated to the same Ru atom,[7] i.e. configuration II of Figure 5. However, it is now known that a value of −11.8 ppm may also be attributed to a bridging hydride.[28]

Moreover, a high-resolution ^{1}H-NMR spectrum of **2a** showed the presence of a small coupling (about 0.5 Hz) between the hydride signal at −11.8 ppm and the signal of the η^2-coordinated N=CH moiety. The presence of such a coupling can be explained far better by structure I than by structure II (Figure 5). A similar coupling between a hydride and the η^2-coordinated N=CH moiety has been observed for $H_2FeRu(CO)_5(^iPr\text{-}Pyca)$[27] and $HRu_2(Cl)(CO)_5(^iPr\text{-}DAB)$.[29] In the latter case configuration II has been confirmed by a single-crystal X-ray structure determination.

Further evidence that one of the hydride ligands occupies a bridging position was obtained from a combination of proton-coupled ^{13}C-NMR spectra and heteronuclear ^{1}H-^{13}C correlations. Two carbonyls, which from the presence of a coupling with the η^2-CH=N proton were identified as coordinated to Ru(1) (Figure 5), also showed a large coupling with the hydride signal at −11.8 ppm (7 and 22 Hz, respectively), which suggests that a bond between Ru(1) and this hydride is present. Moreover, the same coupling pattern was observed for $HRu_2(Cl)(CO)_5(^iPr\text{-}DAB)$[29] for which the presence of a bridging hydride (i.e. like structure I of Figure 5) has been confirmed by X-ray crystallography.

Reactions of $H_2Ru_2(CO)_5(^iPr\text{-}DAB)$ (2a) with H_2 and D_2. An interesting reaction involves the treatment of $H_2Ru_2(CO)_5(^iPr\text{-}DAB)$ (**2a**) with D_2 at 60 °C, which yielded $D_2Ru_2(CO)_5(^iPr\text{-}DAB)$ (**2a′**) in about 4 h. The reaction is reversible since **2a′** with H_2 afforded **2a**. ^{1}H-NMR showed that the bridging hydride, resonating at −11.8 ppm, exchanged much faster than the terminal hydride at −7.8 ppm. Using high-pressure NMR techniques it was shown that, whereas the signal at −11.8 ppm gradually decreased, the signal at −7.8 ppm slowly changed from a doublet to a triplet owing to coupling with D ($J_{H\text{-}D}$ = 3.4 Hz). From these observations it can be concluded that the reaction does not proceed via a simple reductive elimination of H_2 followed by a an oxidative addition of D_2.

In the first instance it would not be expected that it is the bridging hydride ligand that exchanges more rapidly. However, in the case of the isostructural $HRu_2(Cl)(CO)_5(^iPr\text{-}DAB)$,[29] in which the hydride is bridging, a rapid exchange with deuterium was also observed at 70 °C.[29]

A proposed mechanism for the observed H/D exchange reaction of the bridging hydride is shown in Scheme II. It is suggested that the DAB ligand changes its coordination mode from a 6e σ-N, μ_2-N′, η^2-C=N′ bridging to a 4e σ-N′ bonding mode, thereby creating an open site at Ru(1) which may be filled by a η^2-D_2-bonded group close to the bridging hydride (**X2**). It might well be that an HD_2 unit is formed in the transition state[30,31] (**X4**), after which expulsion of HD would lead to $H(\mu_2\text{-}D)Ru_2(CO)_5(^iPr\text{-}DAB)$, which reaction, for reasons of microscopic reversibility, probably proceeds via intermediates **X3′** and **X2′**. Models have shown that Ru(1) indeed offers the most favorable space for attack, while, for steric reasons, Ru(2) is less suitable, which would rationalize the much lower rate of H/D exchange at the terminal hydride on Ru(2). Like Bianchini et al.[31] we cannot discriminate between the

(28) In general, hydride ligands on a bridging position have been observed upfield from −15 ppm. However, it is now clear that there are exceptions to this empirical rule: (a) Reference 5. (b) Reference 36. (c) Zoet, R.; Goubitz, K.; Jansen, G.; Koten van, G.; Vrieze, K.; Stam, C. H. *Organometallics* **1988**, *7*, 1565.

(29) Kraakman, M. J. A.; Elsevier, C. J.; Haar de, V. W.; Spek, A. L.; Vrieze, K. *Inorg. Chim. Acta*, in press.

(30) (a) Bianchini, C.; Peruzzini, M.; Zanobini, F. *J. Organomet. Chem.* **1988**, *354*, C19. (b) Chaudret, B.; Commenges, G.; Jalon, F.; Otero, A. *J. Chem. Soc., Chem. Commun.* **1989**, 210. (c) Heinekey, D. M.; Payne, N. G.; Sofield, C. D. *Organometallics* **1990**, *9*, 2643. (d) Antinolo, A.; Chaudret, B.; Commenges, G.; Fajardo, M.; Jalon, F.; Morris, R. H.; Otero, A.; Schweltzer, C. T. *J. Chem. Soc., Chem. Commun.* **1988**, 1210.

(31) An exchange between a hydride and D_2 to a deuteride and HD was observed before, and an H_3-like intermediate has been proposed: Bianchini, C.; Perez, P. J.; Peruzzini, M.; Zanobini, F.; Vacca, A. *Inorg. Chem.* **1991**, *30*, 279.

possible structures through which the hydride and the D_2 are believed to exchange, i.e. the closed H_3 unit (Scheme II, **X4**) or the open H_3 unit (see ref 31).

When the temperature was increased to 90 °C the reaction of $H_2Ru_2(CO)_5$(^{i}Pr-DAB) (**2a**) with H_2 afforded $H_2Ru_2(CO)_5$(^{i}PrNCH$_2$CH$_2$N^{i}Pr) (**3a**) and $Ru_2(CO)_6$(^{i}PrNCH$_2$CH$_2$N^{i}Pr) (**4a**). A separate experiment showed that the conversion from **3a** to **4a** proceeds under the conditions used during the hydrogenation reaction, thus strongly suggesting that **3a** is the initial product, while **4a** results from **3a** and CO, which is formed by some decomposition of **3a** (Scheme I).

Instead of using **2a** as the starting complex one may also commence with $Ru_2(CO)_6$(^{i}Pr-DAB) (**1a**) or $Ru_2(CO)_5$(^{i}Pr-DAB).[7,21] However, IR spectroscopy showed in all cases that **2a** is formed first, before the hydrogenation reaction started, indicating **2a** is a key intermediate in the hydrogenation process. However, it was found that the product distribution strongly depended on the starting complex and on the reaction conditions used. In general it can be said that the presence of a relative large amount of carbon monoxide in the reaction mixture leads to the formation of more **4a** relative to **3a**, as would be expected. At first sight this observation seems to be a logical consequence, since for the conversion of **3a** to **4a** 1 equiv of carbon monoxide is required, which suggests that the conversion from **3a** to **4a** would proceed more easily in the presence of carbon monoxide. However, a separate experiment showed that the presence of carbon monoxide does not have an accelerating effect on this conversion, which may be rationalized by assuming that the reductive elimination of H_2 from **3a** is the rate-determining step in the conversion from **3a** to **4a**.

When the hydrogenation reaction was performed in the presence of carbon monoxide, it appeared that the hydrogenation reaction was completely inhibited. This inhibiting effect has also been observed for the heteronuclear FeRu system,[27] which was explained by assuming that the carbon monoxide occupies the open site which is created by rupture of the η^2-C=N to metal bond. This inhibiting effect also explains the influence of carbon monoxide on the product distribution since in the presence of traces of carbon monoxide longer reaction times are needed to reach completion; during this time more **3a** may be converted to **4a**, which explains the change in product distribution when varying the starting complex or the reaction conditions.

The reaction of $Ru_2(CO)_6$(^{i}Pr-DAB{H,Me}) (**1b**) with H_2 at 90 °C proceeded similarly. First $H_2Ru_2(CO)_5$(^{i}Pr-DAB{H,Me}) (**2b**) is formed, which at 90 °C converted to $H_2Ru_2(CO)_5$(^{i}PrNC(H)(Me)CH$_2$N^{i}Pr) (**3b**) and $Ru_2(CO)_6$(^{i}PrNC(H)(Me)CH$_2$N^{i}Pr) (**4b**). However, **3b** is rather unstable with respect to **4b**, as **3b** is much more easily converted to **4b** than **3a** to **4a**. One may guess at this relative instability of **3b**. It might be that the instability of **3b** is due to a steric hindrance between the methyl group of the central C–C moiety and the terminal hydride, provided the methyl group is positioned at the Ru(CO)$_2$(H) side of the molecule. Unfortunately we have no spectroscopic evidence for this suggestion. Circumstantial evidence is provided by the fact that in **3a** the terminal hydride is only 2.80 Å away from the closest H atom of the C_2H_4 moiety. If in this moiety one H atom on the Ru(CO)$_2$(H) side of the molecule is substituted, the thermal instability of **3b** might be rationalized.

Intriguing results have been obtained when D_2 was employed instead of H_2. An interesting reaction involves the treatment of $D_2Ru_2(CO)_5$(^{i}Pr-DAB) (**2a′**) with D_2 at 90 °C, resulting in reduction of the C_2H_2 moiety with formation of **3a′** and **4a′**. The ^{1}H-NMR of the product **3a′** showed to our surprise that less than one proton (generally between 0.5 and 1 proton) is present on the C_2 moiety whereas two protons would be expected. On the other hand, a substantial amount of proton intensity was observed at the position at the deuteride side at −7.9 ppm, which appeared as a broad triplet, probably due to coupling with the D atom at the other deuteride site. The same features were found for **4a′**, which was formed from **3a′** by heating.[32,33] Also the reaction of **1b** with D_2, which afforded **4b′**, showed for **4b′** hardly any proton intensity on the positions of H_1, H_2, and H_3 (Figure 4), whereas the ^{2}H-NMR spectrum indicated that deuterium is present on the H_1, H_2, and H_3 positions with roughly identical intensities. The obvious conclusion is that the reduction of the central C_2H_2 unit of the DAB ligand is not stereoselective, in sharp contrast to the reported stereoselective trans addition of two D atoms to the C_2H_2 unit of FeRu(CO)$_6$(^{i}Pr-DAB).[6]

Since the H/D exchange of the hydride/deuteride positions of complexes **2** with D_2/H_2 was shown to be more facile than the reduction of the DAB ligand, it proved to be impossible to reduce the DAB ligand of **2a** with D_2 or to reduce the DAB ligand of **2a′** with H_2.[34] It is important to note that no H/D exchange of the bridging hydride/deuteride with D_2/H_2 occurs for the compound **3a** (Experimental Section). This observation agrees very well with the proposed mechanism (Scheme II), since it is much more difficult to create an empty coordination site on **3a** than on **2a** as no metal–η^2-C=N coordination is present in **3a**.

Mechanistic Aspects. An important result is that the hydrogenation reactions are completely inhibited by the presence of free CO (Experimental Section), indicating that CO is a good reagent to probe the reactive site of the ruthenium dihydride compounds **2**, which are the starting compounds in all cases. The proposed mechanism (Scheme III) involves in the first step the creation of an open coordination site by rupture of the Ru(1)–η^2-C=N bond, thus leading to intermediate **X5**. From recent work involving the analogous heteronuclear systems[27] it appeared that the creation of such an open site in this way is a plausible assumption. In the presence of carbon monoxide a carbonyl ligand may coordinate to this open site, thus inhibiting the hydrogenation reaction. However, in the absence of this inhibiting agent D_2 may coordinate to the site on Ru(1) vacated by the originally η^2-C=N-bonded imine unit, followed by the formation of inter-

(32) Although it is clear that only one of the hydrides is involved in the exchange process with the atoms of the partially hydrogenated DAB ligand, we have not been able to obtain spectroscopic evidence for the assumption that it is the bridging hydride that is involved in this process and not the terminal hydride, since, in contrast to complex **2**, we have not been able to determine which signal belongs to the bridging hydride and which signal belongs to the terminal hydride in complex **3**. However, this assumption was supported by studying the analogous halogenated system, in which the terminal hydride has been exchanged for a halide, and in which the bridging hydride also proved to be involved in an exchange process with the atoms of the partially hydrogenated DAB ligand during the hydrogenation reaction (see ref 29).

(33) Unfortunately, we have not been able to separate **3a′** and **4a′**. Although the presence of broadened signals belonging to **4a′** complicated the precise integration of the signals of **3a′**, it appeared that only little intensity was present for the multiplet around 2.57 ppm, while the integral of the multiplet around 2.85 ppm indicated in addition to the two ^{i}PrCH protons very little proton intensity on the C_2H_4 moiety. The shortage of proton intensity on the C_2H_4 moiety became clear after converting the mixture of **3a′** and **4a′** to complex **4a′** exclusively, by heating the product mixture.

(34) It was indeed observed that treatment of **2a′** with H_2 at 90 °C gives the same result as treatment of **2a** with H_2; i.e., a completely nondeuterated product was obtained due to a rapid conversion of **2a′** to **2a** before the hydrogenation reaction started.

Scheme III. Proposed Mechanism for the Deuteration of Complex 2a'/2b'

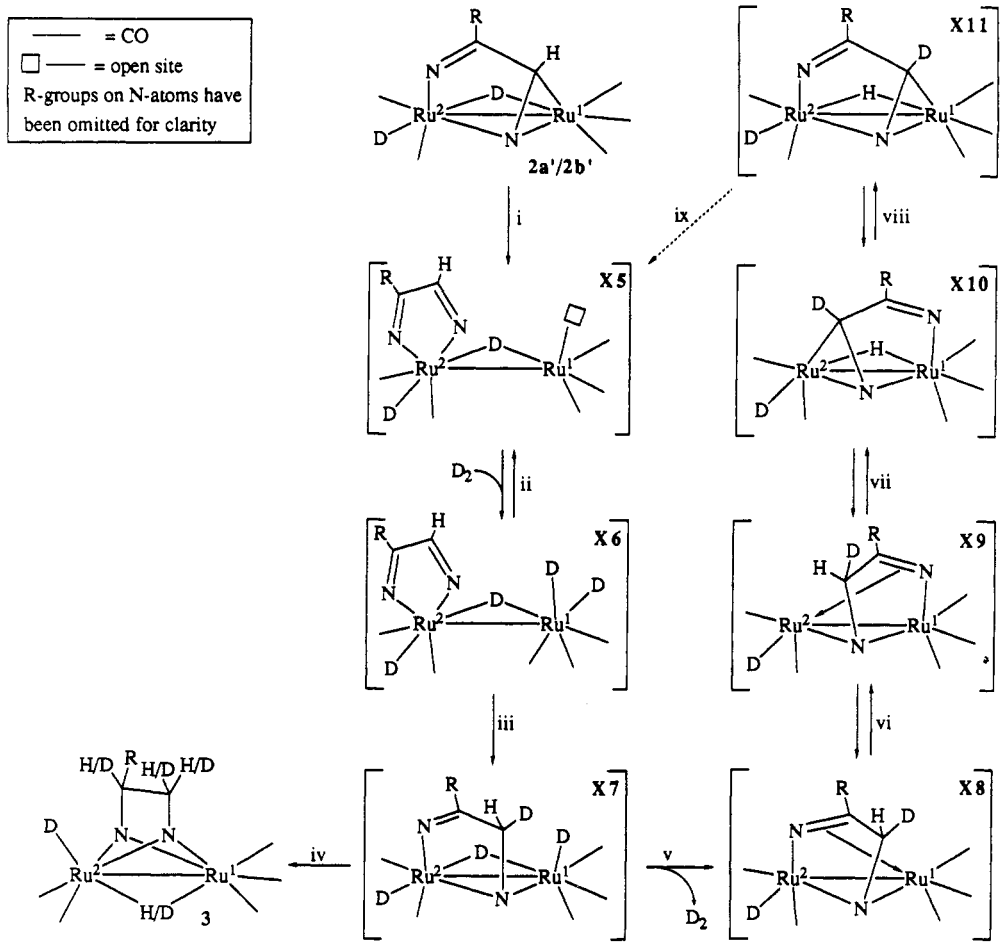

mediate **X6**. It should be noted that a structure like **X3** or **X4** (compare Scheme II) may also be involved at this stage of the reaction. Subsequently D transfer might occur directly to one imine C atom. There are precedents for such a transfer reaction,[4-6] which were proposed to proceed via a polar four-center transition state[6] or via a single electron transfer mechanism.[5]

For the analogous heteronuclear FeRu system it was suggested that from **X7** a hydride transfer to the other metal occurred at this stage, followed by a rapid transfer to the second imine moiety. This may occur in our case as well (iv), leading to the deuterated complex. **3a'**. However, we propose that for the system presented here an alternative route is possible. Reductive eliminative of D_2 accompanied by η^2-C=N coordination to Ru(1) will lead to **X8** (v). The structure of **X8** is analogous to that of $Ru_2(CH_3C{=}C(H)CH_2N^iPr)$[35,36] in which the enyl–amido ligand is coordinated in the same way as the partially reduced ligand in **X8**, as was confirmed by X-ray crystallography. It has been shown that the enyl–amido ligand is involved in a windshield-wiper type of motion, which process is outlined in Figure 6.

Likewise **X8** might change to the structurally analogous **X9** (vi). Subsequent decoordination of the η^2-C=N bond in **X9** will provide an empty coordination site on Ru(2), after which C–H activation may occur affording **X10** (vii). This shift of H from C to the bimetallic unit is analogous to a similar shift observed for $Ru_2(CH_3C{=}C(H)CH_2N^iPr)$.[35,36] This intermediate will now rapidly isomerize to

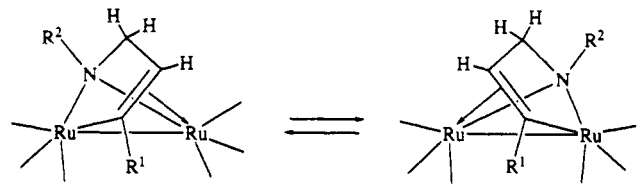

Figure 6. Fluxional behavior observed for $Ru_2(CO)_6[R^1C{=}C(H)C(H)_2NR^2]$ (taken from ref 35).

a conformation analogous to that of the starting compound **2a'**, i.e. to intermediate **X11** (viii). This isomerization may be understood by a stronger η^2-C=N coordination to Ru(1) as compared to Ru(2) since, as a result of the oxidation states of the two metals, π-back-bonding from Ru(1) will be stronger than π-back-bonding from Ru(2). Isomerizations like the one suggested here (viii) have been reported before.[37,38]

The cycle may now start again, and hence, the second imine moiety may also become labeled. From this cycle it may now also be understood that H atoms also appear in the bridging hydride site of **3**, whereas the terminal hydride site remains unaffected, as is indeed observed. It should be clear that due to exchange with D_2 gas, the total proton content in the product is lower than in the starting

(35) Mul, W. P.; Elsevier, C. J.; Polm, L. H.; Vrieze, K.; Zoutberg, M. C.; Heijdenrijk, D.; Stam, C. H. *Organometallics* **1991**, *10*, 2247.

(36) Mul, W. P.; Elsevier, C. J.; Leijen van, M.; Vrieze, K.; Smeets, W. J. J.; Spek, A. L. *Organometallics* **1992**, *11*, 1877.

(37) Zoet, R.; Goubitz, K.; Halen van, C. J. G.; Koten van, G.; Vrieze, K. *Inorg. Chim. Acta* **1988**, *149* (2), 193.

(38) Muller, F.; Koten van, G.; Kraakman, M. J. A.; Vrieze, K.; Zoet, R.; Duineveld, C. A. A.; Heijdenrijk, D.; Stam, C. H.; Zoutberg, M. C. *Organometallics* **1989**, *8*, 982.

compound, since H atoms originating from the DAB ligand may first exchange with the D atom on the bridging deuteride position and subsequently be transferred to the gas atmosphere. It is again interesting to note that as soon as the final product is formed no H/D exchange occurs anymore between the hydride/deuteride atoms of **3a**/**3a'** with the D_2/H_2 gas.

It is important to note that, according to the mechanism presented in Scheme III, the terminal hydride does not undergo H/D exchange with the H atoms of the DAB ligand, which agrees with the NMR data.[32] According to the presented mechanism (Scheme III) the terminal hydride does not participate at all in the reduction process. This agrees with the observation that the terminal hydride can be exchanged for a chloride atom without significant influence on the course of the reduction process.[29]

The lack of stereoselectivity is clearly due to the presence of relatively long-lived hydride intermediates which are not operative during the reduction of the FeRu systems, the mechanisms of which we have reported in separate articles.[6,27]

Preparation of Complexes 5. Recently the reaction of the heteronuclear complex $FeRu(CO)_6(^iPrNCH_2CH_2N^iPr)$ with PPh_3 to form $FeRu(CO)_5(PPh_3)(^iPrNCH_2CH_2N^iPr)$[27] has been reported, which reaction was shown to be reversible. In order to be able to compare the Ru_2 system described here a similar reaction was performed starting from **4a,b**.

Although thermally (toluene, 80 °C) the reaction of **4a,b** with triphenylphosphine led to the formation of complexes **5**, this does not provide a favorable route, since a large excess of triphenylphosphine is required, long reaction times are needed, and the reaction is accompanied by a substantial amount of unknown side reactions. However, a clean and rapid reaction occurred by treatment of **4a,b** with Me_3NO in toluene at −60 °C and subsequent addition of 1 equiv of PPh_3. Upon addition of Me_3NO at first an intermediate **X1** is formed, for which a plausible formulation is $Ru_2(CO)_5(NMe_3)(^iPrNC(H)(X)CH_2N^iPr)$ (X = H; X = Me) (Scheme I). The IR spectroscopic data of **X1** are included in Table VIII.

Treatment of **X1** with carbon monoxide led to an instantaneous conversion to the starting complexes **4**. Intermediate **X1** is not stable at room temperature and gives decomposition, accompanied by the formation of **4**. Upon addition of phosphine complexes **5a,b** were isolated in high yields.

Due to the presence of the Me group in the case of **4b**, the conversion to **5b** may in principle lead to the formation of two isomers. From spectroscopic data it was concluded that only one isomer is formed. Since steric effects of the Me group on the carbonyl ligands in **3b** and **4b** is important (vide supra), we think that one of the carbonyls on the methylated side of the molecule is the weakest coordinated. We therefore suggest that **5b** contains a phosphine ligand on the same side of the molecule as the Me group (Figure 4 and Scheme I).

Concluding Remarks. A fascinating difference between the hydrogenation of the Ru_2 systems (ref 29 and this paper) and the FeRu systems[6,27] studied is that in the latter case use of D_2 leads to stereoselective trans addition of two D atoms to the central C–C bond of the coordinated DAB ligand, whereas in the case of the Ru_2 systems the D atoms are randomly substituted on the C_2 moiety. Furthermore, more than two D atoms arrive on the C_2 unit, whereas at the same time H, originally bonded in the former C_2H_2 unit, has been transferred to the bridging deuteride position of e.g. $DRu_2(X)(CO)_5(^iPr\text{-}DAB)$ (X = H, Cl) (Scheme III and ref 29).

Therefore, at this stage it is of interest to address ourselves to the question of why these systems differ. In our view the main cause of difference lies in the existence of stable hydride/deuteride intermediates, like $H_2Ru_2(CO)_5(^iPr\text{-}DAB)$ (**2a**), in the case of Ru_2 complexes, whereas these species have been observed for the FeRu compounds with DAB ligands.[6] Up to intermediate **X7** of Scheme III the mechanism is similar to the mechanism proposed for the FeRu systems.[6,27] However, in the case of Ru_2 after **X7** H/D exchange may occur between the C_2 moiety and the bridging hydride/deuteride, which is not possible for the FeRu system. In the FeRu case a cycle like that presented in Scheme III from **X8** to **X11** is not feasible.

Acknowledgment. The authors wish to thank Dr. H.-W. Frühauf for his interest and helpful suggestions. The authors also thank J.-M. Ernsting for advice and practical assistance during the collection of the NMR data. This work was supported in part (A.L.S.) by the Netherlands Foundation for Chemical Research (SON) with financial aid from the Netherlands Organization for Scientific Research (NWO). The X-ray data were kindly collected by A. J. M. Duisenberg.

Supplementary Material Available: Tables of anisotropic thermal parameters, all H-atom parameters, bond lengths, and bond angles and figures showing thermal ellipsoid plots of **3a** and of both residue molecules of **4a** (13 pages). Ordering information is given on any current masthead page. Listings of observed and calculated structure factors of **3a** (26 pages) and **4a** (36 pages) can be obtained from A.L.S.

OM920321M